Forming of magnesium alloy cup using friction heated punch

HARADA Yasunori[1,a *] and TAKAHARA Taiki[2,b]

[1]Graduate School of Engineering, University of Hyogo, C229, 2167 Shosya, Himeji, Hyogo 6712280, Japan

[2]Graduate Student of Engineering, University of Hyogo, C230, 2167 Shosya, Himeji, Hyogo 6712280, Japan

[a]harada@eng.u-hyogo.ac.jp, [b]takaharak059@gmail.com

Keywords: Sheet Forming, Deep Drawing, Drawn Cup, Magnesium Alloy, Friction Heating, Thermal Conductivity, Dissimilar Materials

Abstract. In deep drawing of aluminum and magnesium alloys, it is known that many alloys are difficult to form at room temperature. In particular, many commonly used magnesium alloys are very difficult to form at room temperature. To improve formability, warm processing is used. However, the problem is that the mold requires heating and cooling equipment and its control equipment. In the present study, we attempted warm deep drawing using frictional heat generation. To heat the punch itself, a frictional heat generation structure was incorporated inside the punch. The materials of the friction heater jig were several kinds of stainless steel and alloy steel tools. The relationship between the heat generation temperature of the frictionally heated punch and the working time was investigated. In addition, the amount of wear due to friction of each jig was investigated. It was found that sufficient working temperatures were obtained in the friction-heated combination of austenitic stainless steel and alloy tool steel. It was also found that good formability of the deep-drawn cup was obtained in warm deep drawing using the prototype friction heated punch.

Introduction

In recent years, efforts have been made to improve the fuel efficiency of next-generation vehicles such as electric vehicles, hybrid vehicles, and fuel cell vehicles in order to reduce carbon dioxide emissions. In the case of automobiles, the weight of the vehicle body tends to increase due to the expansion of equipment such as electronic parts. In addition, rapid progress is being made in the combination of multiple materials with different properties, in other words, the use of multi-materials to achieve higher strength and lighter weight [1]. In the case of vehicle bodies for transportation machines such as automobiles and aircraft, the use of resins and light metals instead of steel materials is being promoted in order to reduce weight [2, 3]. Aluminum (Al) alloys and magnesium (Mg) alloys are attracting attention as representative light metals [4, 5]. Cast or extruded parts are used for many Al alloys and Mg alloys. Recently, from the viewpoint of mass production, material yield, and thinning of products, it has been desired to apply press processing to sheet materials [6]. However, it is known that some alloys are difficult to process at room temperature [7, 8]. For example, in the case of Mg alloys processed by rolling or extrusion, it is difficult to form them due to the characteristic texture formed during deformation [9, 10]. Currently, press processing is often used in the manufacture of automobiles using parts that make up automobiles such as bodies and doors [11]. Press forming has been used for a long time as a typical plastic working technique. This technique has relatively high productivity because it allows products to be produced in large quantities with fewer steps. Furthermore, by changing the mold, it can be processed into multiple shapes such as shearing and bending. One of these processing methods is deep drawing. This is a technology in which a blank metal sheet is placed in a metal mold called a die, and a punch tool is used to apply a predetermined load to form a seamless three-dimensional container. Although it is known as a severe processing method in press processing, it is relatively suitable for mass production. It is widely used in industrial products such as automotive parts such as sensor cases and battery cases, and in daily necessities such as beverage cans and cooking pots [12, 13]. As mentioned above, however, many Al alloys and Mg alloys have lower ductility and poor formability than steel materials. In particular, in the case of Mg alloys, many alloys are difficult to process at ambient temperature, with the exception of beta-type alloys [14] and microstructurally controlled alloys [15, 16]. For this reason, it is currently very difficult to form the material using cold deep drawing. One method to improve forming performance is warm deep drawing [17]. This process heats the flange before forming to reduce deformation resistance, thereby improving the formability of deep drawing. Formability is also improved by increasing deformation resistance and strength by cooling the part that contacts the punch shoulder. In the case of warm forming, however, the current problem is that a control device with a heating and cooling structure is required for the forming mold and the high cost associated with such equipment.

In the present study, we focused on the frictional heat generated during friction stir welding (FSW) and friction joining (FJ). In FSW and FJ technology, this is a technology in which materials softened by frictional heat are stirred and welded. Many studies have been reported on joining dissimilar materials [18, 19]. In the case of steel materials, it is known that the temperature generated by friction is over 900ºC [20]. In order to heat the metal punch itself, a frictional heat generation structure was incorporated inside the punch. In other words, a friction heat generating jig made of different metals was built inside the punch. Warm deep drawing was attempted using the frictional heat generated by the rotation of the jig. The relationship between the frictionally heated punch temperature and working time was investigated. Warm deep drawing was also performed using a friction heated punch.

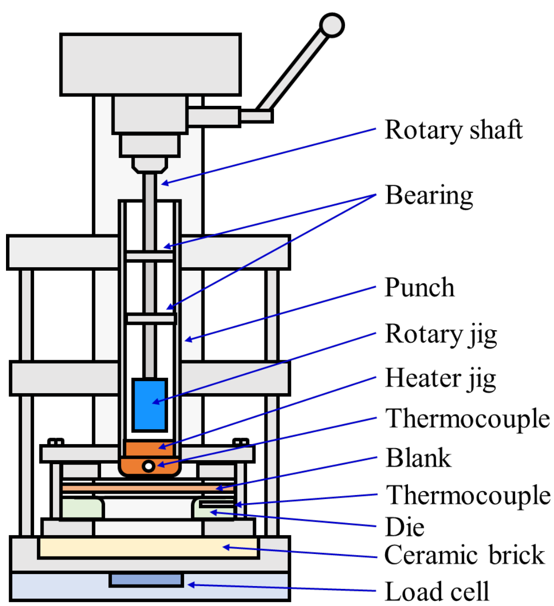

Fig. 1. Deep drawing method by using friction heating.

Experimental procedures

The prototype punch was heated by frictional heat. A deep drawing equipment consisting of punch and die was installed on a drilling machine. A schematic illustration of the warm deep drawing equipment using frictional heat is shown in Fig. 1. The punch is heated by the spindle of the drilling machine. At the tip of the punch, when a predetermined temperature is reached, the spindle is lowered by rotation of the drilling machine handle. The upper part of the rotary shaft connected to

Materials Research Proceedings 44 (2024) 340-349 https://doi.org/10.21741/9781644903254-36

the rotary jig was attached to the gripping section of the drilling machine. The rotational speed ranged from 2400 to 2800 rpm. The rotating shaft was fixed by two bearings installed inside the punch. The temperature generated by frictional heating was measured by several thermocouples. The measurement locations were near the heater jig and the die shoulder radius.

The material of the rotary jig was tool steel or stainless steel. The heater jig was the same alloy tool steel used for the die. These jigs used are material grades and designation defined in JIS (Japanese Industrial Standards) standards. In the deep drawing process, the blanks used were Al alloy A5052 and Mg alloy AZ31. The blanks were 35 mm in diameter and 0.5 mm thick. The punch was a commercially available stainless steel SUS304 pipe. SUS304 is chromium-nickel austenite stainless steels. This steel is a material grade and designation defined in JIS G4303 standard. It was 160 mm long, with outer and inner diameters of 20 mm and 16 mm, respectively. The punch had a diameter of 20 mm and a shoulder radius of 3 mm. The die had a hole diameter of 21 mm and a shoulder radius of 4 mm. The lubricant was a heat-resistant molybdenum disulfide-based work oil. The clearance between the punch and the die was 0.5 mm. Table 1 shows working conditions in friction heating.

Table 1. Working conditions in friction heating.

Rotary jig	Alloy steel	SUP9 (spring steel, Cr-Mg steel), 299 HV
		SUJ2 (bearing steel, high-carbon Cr steel), 318 HV
		SCM440 (Cr-Mo steel), 326 HV
		SKS3 (Mn-Cr-W steel), 210 HV
	Alloy tool steel	SKD11 (cold work tool steel), 232 HV
		SKD61 (hot work tool steel), 220 HV
		SKH51 (high-speed tool steel), 231 HV
	Stainless steel	SUS303 (austenite stainless steel), 300 HV
		SUS304 (austenite stainless steel), 188 HV
		SUS310S (austenite stainless steel), 237 HV
		SUS316L (austenite stainless steel), 249 HV
		SUS403 (martensitic stainless steel), 206 HV
		SUS430 (ferritic stainless steel), 188 HV
		SUS327L1 (duplex phase stainless steel), 273 HV
		SUS630 (precipitation hardening steel), 415 HV
Heater jig	Alloy tool steel	SKD11 (cold work tool steel), 232 HV
		SKD61 (hot work tool steel), 220 HV
		SKH51 (high-speed tool steel), 231 HV
Rotating velocity		2400 - 2800 rpm
Surface roughness of worked surface (by polishing paper, particle size: d)		Sa*: 0.33 mm, Sz**: 5.97 mm (abrasive paper count: #240, d: 0.08 mm)
Load force of rotary jig		200 - 400 N

* Sa (ISO 25178) is a parameter that extends an arithmetic mean height Ra to a surface.
** Sz (ISO 25178) is the extension of a maximum height Rz to a surface.

After friction processing, the surface state of the rotary jig and heater jig that generated heat was observed with a digital microscope. The wear depth was also measured for the rotary jig and the heater jig after processing. The wear depth was defined as the dimensional change in the depth direction from the surface before and after processing. The maximum length before and after friction heating was measured with a digital micrometer in the rotary and the heater jigs.

Materials Research Proceedings 44 (2024) 340-349 https://doi.org/10.21741/9781644903254-36

Results and Discussions

The relationship between the punch temperature heated by friction and the processing time of friction was investigated. The temperature of the heater jig was measured when the rotary jig was in contact with the heater jig while rotating. The relationship between the temperature and working time of heater jig SKD11 is shown in Fig. 2. The rotary jig was alloy steel type (a) and stainless steel type (b). The broken line in the figure indicates the temperature at which the rotary jig stopped rotating, which is 350°C. In the warm forming of light metals, it is generally known that the forming limit is greatly improved when the metal is heated to approximately 300°C [21, 22]. In the preliminary test, the heater jig reached a temperature of more than 500°C after a few minutes due to friction with the rotary jig. Since a heating temperature of approximately 300°C was sufficient for forming light metals, the rotation of the rotary jig was stopped when the heating temperature reached 350°C. The temperature of heat generated by friction was 350ºC or higher in all rotary jigs. After the rotary jig stopped rotating, the heat temperature increased. When the rotary jig was made of stainless steel, the maximum temperature of the heater jig was approximately 400°C . Moreover, the time during which the temperature was maintained at 350°C or higher was long, i.e., 100 s or longer. This is because the thermal conductivity of stainless steel is lower than that of other steel materials [23].

The effect of the material of the heater jig on heat generation was investigated. When the material of the heater jig was changed, there was little effect on the relationship between the frictional heat-generating temperature and the processing time. The maximum temperature of the stainless steel type rotary jig was found to be higher, and the retention time above 350°C was also longer. The relationship between heat generation temperature and rotation time is shown in Figs. 3 and 4, respectively.

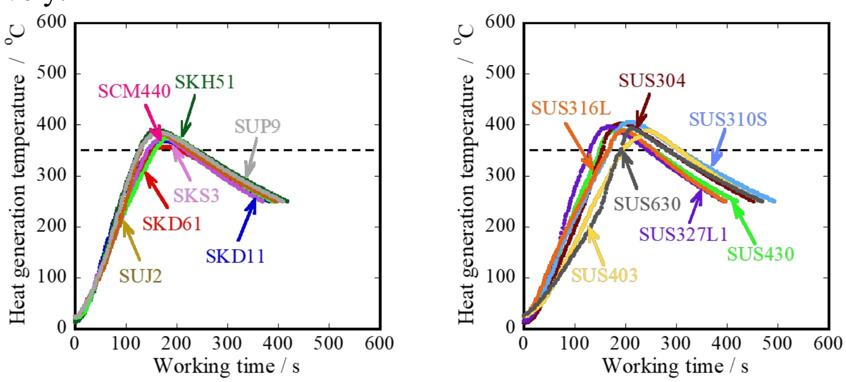

(a) Rotary jig: alloy steel type (b) Rotary jig: stainless steel type

Fig. 2. Variations of heat generation temperature with working time for heater jig SKD11.

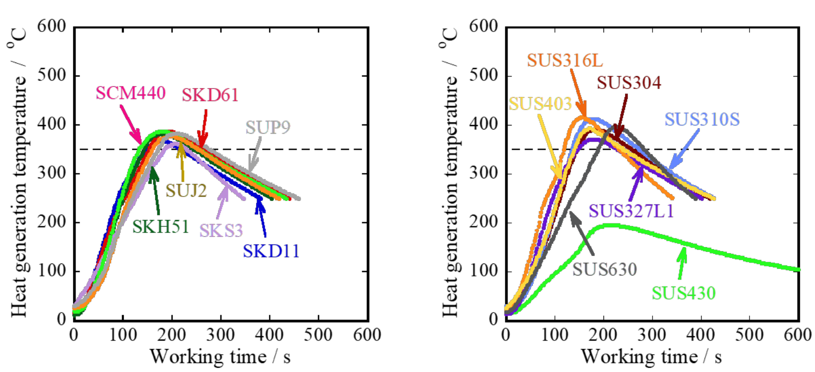

(a) Rotary jig: alloy steel type (b) Rotary jig: stainless steel type

Fig. 3. Variations of heat generation temperature with working time for heater jig SKD61.

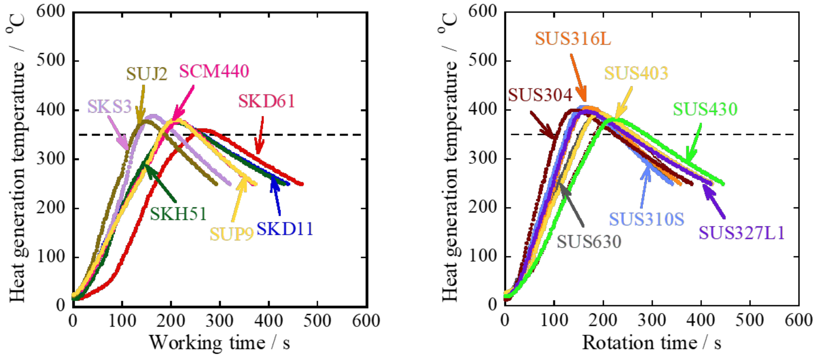

(a) Rotary jig: alloy steel type (b) Rotary jig: stainless steel type

Fig. 4. Variations of heat generation temperature with working time for heater jig SKH51.

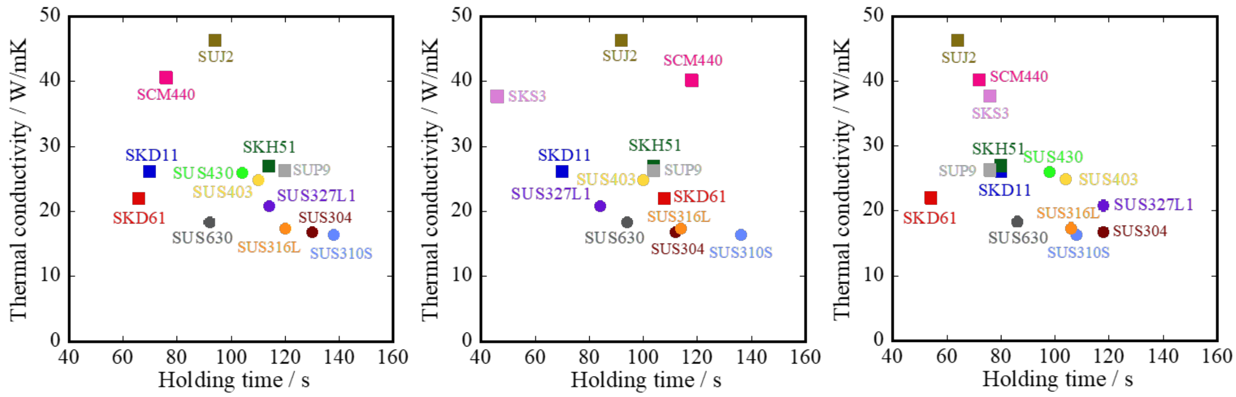

(a) Heter jig: SKD11 (b) Heater jig: SKD61 (c) Heater jig: SKH51

Fig. 5. Relationship between thermal conductivity and holding time of over 350ºC.

Differences in time were observed between different types of rotary jigs in terms of holding time at heating temperatures above 350ºC. In the rotary jigs made of stainless steel, the time to hold the heating temperature above 350ºC was long. This is because the thermal conductivity of stainless steel is smaller than that of other steel materials. Therefore, the relationship between the time for which the temperature is maintained at 350°C and the thermal conductivity was investigated. The relationship between holding time and thermal conductivity in various rotary jigs is shown in Fig. 5. The heater jigs are SKD11 (a) , SKD61 (b) and SKH51 (c). Especially, the holding time of SUS304 and SUS310S was 120 s or longer. In other words, the thermal conductivity of these materials is low. The thermal conductivity of tool steel is approximately 45.1 W/(m-K), while that of stainless steel SUS304 is approximately 16.0 W/(m-K) [24]. Therefore, the use of stainless steel as the rotary jig was found to be effective for heating the punch.

After frictional heating, the surface condition of the rotary and heater jig was observed. The surfaces of the rotary jig SUS304 and heater jig SKH51 after friction processing are shown in Fig. 6. Although traces of friction were observed, no seizure was observed. Similarly, almost no seizure was observed in other combinations of rotary jigs and heater jigs.

The amount of wear on the rotary jig and heater jig after frictional heating was investigated. The amount of wear was defined as the wear depth obtained by measuring the dimensional change of the jig. The wear depth after friction tests on alloy tool steel type (a) and stainless steel type rotary jigs is shown in Fig. 7. The heater jig was SKD11. In the case of rotary jigs made of alloy tool steel, the wear depth for all rotary jigs was less than 0.02 mm. In the case of rotary jigs made of stainless steel, the wear depth was more than 0.02 mm. Due to the low thermal conductivity of stainless steel, heat tends to accumulate in the surface layer. The softening of the surface layer is

Materials Research Proceedings 44 (2024) 340-349 https://doi.org/10.21741/9781644903254-36

thought to have increased the amount of wear. In stainless steel rotary jigs, the wear depth of SUS310S, SUS403, and SUS630 was 0.04 mm or more. The exact reason why the wear amount of the three types of steel was higher is currently unknown.

Similarly, when the heater jig was changed to SKD61 or SKH51, the amount of wear of the stainless steel type jig increased compared to that of the alloy tool steel jig. The wear depth after friction tests on alloy tool steel type (a) and stainless steel type rotary jigs is shown in Fig. 8. The heater jig was SKD61.

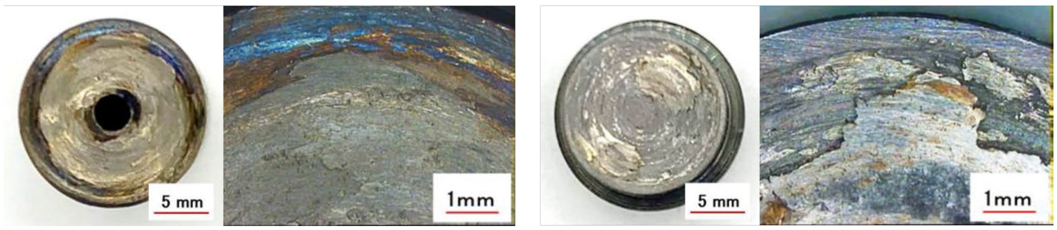

(a) Rotary jig: SUS304 (b) Heater jig: SKH51

Fig. 6. Surfaces of rotary jig and heater jig after friction processing.

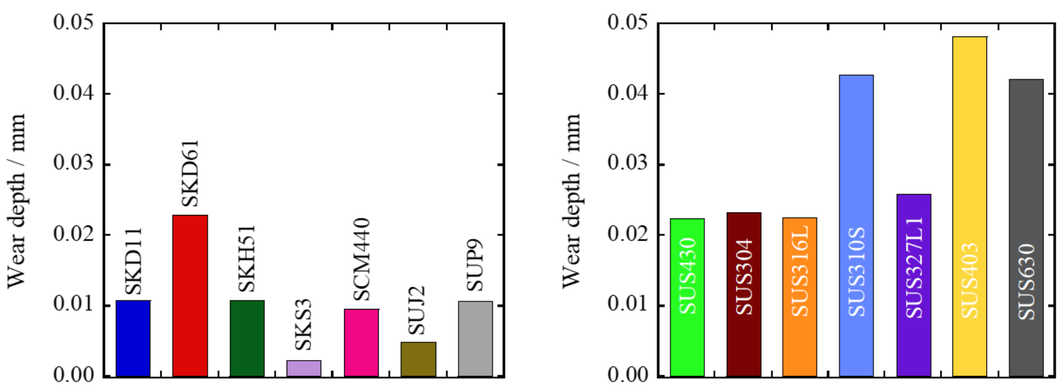

(a) Rotary jig: alloy tool steel type (b) Rotary jig: stainless steel type

Fig. 7. Wear depth of rotary jig relative to heater jig SKD11.

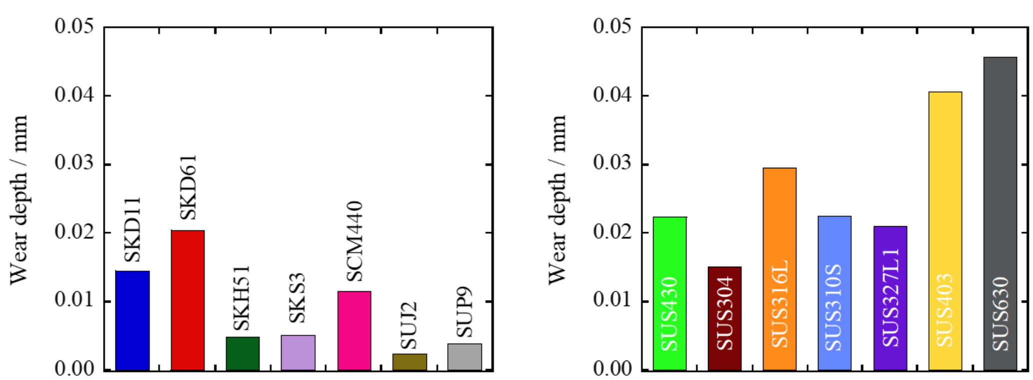

(a) Rotary jig: alloy tool steel type (b) Rotary jig: stainless steel type

Fig. 8. Wear depth of rotary jig relative to heater jig SKD61.

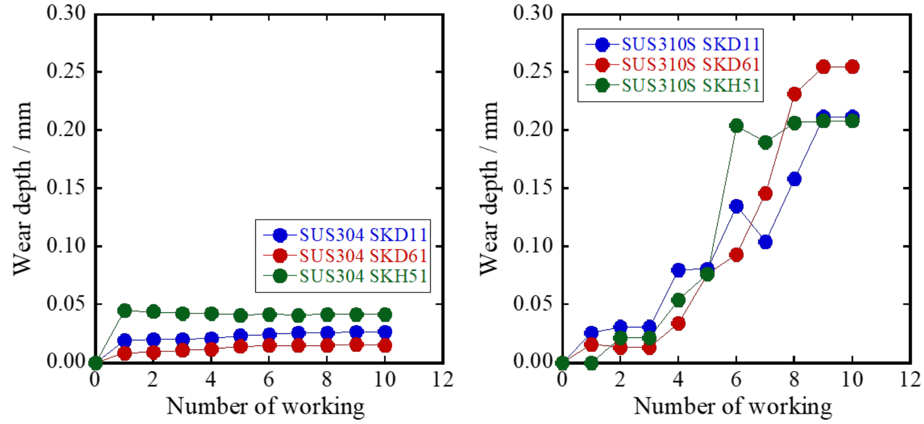

(a) Rotary jig: SUS304 (b) Rotary jig: SUS310S

Fig. 9. Variations of wear depth of rotary jig with number of working.

The effect of the number of friction tests on the wear depth was investigated. The friction test was performed multiple times in succession to measure the amount of wear. The wear depth after multiple friction tests on the stainless steel type rotary jig is shown in Fig. 9. The number of steps in the wear test was 10 times. In the second and subsequent wear depth measurements, the length of the jig before the test was used as the standard. The rotary jig was made of stainless steel SUS304 (a) and stainless steel SUS310S (b). The heating jigs were SKD11, SKD61, and SKH51. In both rotary jigs, the rotary jig was worn in the first test. In the second and subsequent tests, the depth of wear for SUS304 did not change much from the depth of wear in the first test. In the tenth test, the jig wear depth was less than 0.05 mm for the three types of heater jigs. On the other hand, when the rotary jig was made of SUS310S, the wear depth increased significantly after the second test; at the 10th test, the wear depth ranged from 0.20 mm to 0.26 mm. In austenitic stainless steels, the addition of Cr and Ni in SUS310S is higher. The Cr and Ni content in SUS304 is 18 wt.% and 8 wt.%, and that in SUS310S is 20 wt. % and 25 wt. %. When the Ni content is high, the work hardening rate decreases; the work hardening coefficients for SUS304 and SUS310S are approximately 0.44 and approximately 0.34. The reason why the wear of SUS310S jigs is greater than that of SUS304 jigs is because the hardness of the surface layer during friction is lower.

The effect of the material type of the heater jig on the wear depth after multiple friction tests was investigated. There was almost no effect of material on the wear depth of SUS304 and SUS310S rotary jigs.

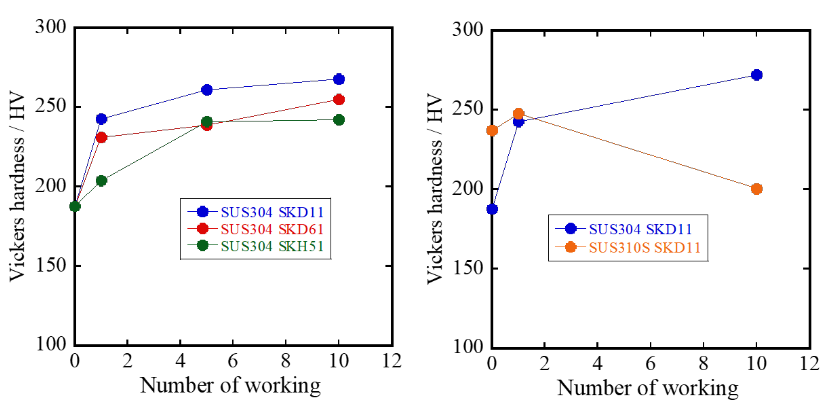

(a) Rotary jig: SUS304 (b) Rotary jig: SUS304, SUS310S

Fig. 10. Variations of Vickers hardness with number of working.

R.T. (4.8 kN) 133 ºC (4.2 kN) R.T. (fractured) 210 ºC (2.9 kN)
(a) Aluminum alloy A5052 (b) Magnesium alloy AZ31

Fig. 11. Appearances of drawn cups by using friction heated punch.

Differences in the depth of wear after multiple friction tests were observed for the SUS304 and SUS310S rotary jigs. The hardness of the surface layer of both jigs after the multiple friction test was examined. The relationship between the hardness of the surface layer of the rotary jig and the number of friction tests is shown in Fig. 10. Each figure shows the change in hardness of the rotary jig SUS304 with respect to three different heater jigs (a) and the change in hardness of two different rotary jigs with respect to the heater jig SKD11 (b). In the rotary jig SUS304 (a), as the number of tests increased, the hardness for the three types of heater jigs also increased. When the number of tests was 10 times, the hardness of the rotary jig was approximately 250 HV. The hardness of the rotary jig was approximately 1.3 times higher than the pre-test hardness. Microstructural observation of the cross section showed that fine microstructures were observed in the surface layer. After the rotation of the rotary jig stopped, recrystallization is thought to have occurred in the worked layer. As the number of tests increased, the area of fine structure expanded. Regarding the rotary jig SUS304 and SUS310S for the heater jig SKD11 (b), the hardness of the rotary jig SUS310S decreased as the number of tests increased. In the surface layer of the rotary jig SUS310S, few areas of fine structure were observed.

Warm deep drawing was performed using the punch heated by frictional heating. The appearances of the drawn cup A5052 (a) and drawn cup AZ31 (b) are shown in Fig. 11. The temperature of the process was measured inside near the shoulder of the die. In the A5052 blank (a), formability was good. The cup could be formed at room temperature, and the warm forming load was reduced. The maximum loads were 4.8 kN and 4.2 kN at room temperature and warm forming. In the AZ31 blank (b), fracture occurred at room temperature due to poor ductility. At warm temperatures, however, the formability was improved. In warm forming, the maximum load was 2.9 kN. The thickness distribution of the warm drawn cups was measured; the maximum reduction in thickness for the A5052 and AZ31 cups was approximately 5 % for both cups.

Summary

Friction heating was performed on several combinations of steel materials using the punch with a built-in friction heater jig. The following results were obtained: (1) When the rotary jig was made of alloy tool steel or stainless steel, a heat generation temperature of 370 to 400ºC was obtained at a rotation time of 180 s; (2) When the rotary jig was made of austenite stainless steel, a holding time of more than 350ºC was obtained for more than 100 s due to low thermal conductivity; (3) No trace of burning was observed on the friction surfaces where the rotary jig and heater jig contact each other; (4) When the rotary jig was made of stainless steel, the depth of wear increased compared to other grades of rotary jigs, but the maximum value was less than 0.1 mm; (5) The proposed method was capable of heating to the punch. Therefore, it was found that there was a possibility to improve the workability of Mg alloys by warm deep drawing.

Acknowledgment

The authors would like to thank Mr. H. Togawa, Material and Manufacturing Center, for advice on experimental equipment. This research was supported in part by a grant from AMADA foundation under grant No. AF-2020016-B3.

References

[1] D. Li, X. Fang, Lightweight design approach of an LFT-metal multi-material vehicle door concept, Automot. Engine Tech. 7 (2022) 385-407. https://doi.org/10.1007/s41104-022-00121-9

[2] I. Turkmen, N.S. Koksal, Investigation of mechanical properties and impact strength depending on the number of fiber layers in glass fiber-reinforced polyester matrix composite materials, Mater. Testing 56 (2014) 472-478.

[3] H. Li, X. Sun, J. Wang, L. Wang, Study of aging stability and precipitation kinetic of the Al-Zn-Mg alloy applied for auto body structures, J. Mater. Res. Tech. 9 (2020) 15575-15584. https://doi.org/10.1016/j.jmrt.2020.11.025

[4] P. Shurkin, G. Scamans, N. Barekar, L. Hou, T. Subroto, C. Barbatti, Phase composition and microstructure of high strength AA6xxx aluminium alloys with nickel additions, Materials Trans. 64 (2023) 398-405. https://doi.org/10.2320/matertrans.MT-LA2022047

[5] A. Kielbus, R. Jarosz, Gating system optimization for EV31A magnesium alloy engine body sand casting, Materials 15 (2022) 4620. http://dx.doi.org/10.3390/ma15134620

[6] K.S. Bhandari, S. Aziz, W.N. Chen, S.J. Li, D.W. Jung, Deformation evaluation of A5052 sheet metal in SPIF process, Mater. Sci. Forum 1084 (2023) 91-95. http://dx.doi.org/10.4028/p-e6768o

[7] R. Comanei, L. Zaharia, R. Chelariu, Damaging prediction of difficult-to-work aluminum alloys during equal channel angular pressing, J. Mater. Eng. Perform. 213 (2012) 287-297. https://ui.adsabs.harvard.edu/link_gateway/2012JMEP...21..287C/doi:10.1007/s11665-011-9904-5

[8] S. Fritsch, S. Hunger, M. Scholze, M. Hockauf, M.F.-X. Wagner, Optimisation of thermo mechanical treatments using cryogenic rolling and aging of the high strength aluminium alloy AlZn5.5MgCu (AA7075), 42 (2011) 573-579. http://dx.doi.org/10.1002/mawe.201100835

[9] E. Tolouie, R. Jamaati, Effect of rolling reduction on the microstructure, texture, and mechanical behavior of AZ91 alloy, J. Mater. Res. Tech. 26 (2023) 7947-7957. https://doi.org/10.1016/j.jmrt.2023.09.119

[10] S.M. Fatemi, H. Paul, A. Hemmati-Hosuri, Microstructure, texture, and instability during superplastic deformation of ECAP-treated AZ31 Mg alloy, Mater. Sci. Tech. 39 (2023) 1661-1669. http://dx.doi.org/10.1080/02670836.2023.2180594

[11] P. Kaczynski, M. Skwarski, K. Jaskiewicz, Development of the technology for press-forming of energy-absorbing elements made of 7075 aluminum alloy, J. Manuf. Process. 50 (2020) 676-683. https://doi.org/10.1016/j.jmapro.2020.01.023

[12] F. Han, R. Radonjic, New approach for wrinkle prediction in deep drawing process, Key Eng. Mater. 639 (2015) 459-466. https://doi.org/10.4028/www.scientific.net/KEM.639.459

[13] C. Lee, G. Park, C. Kim, Design of Type 3 High-Pressure Vessel Liner (Al 6061) for Hydrogen Vehicles, J. Pressure Vessel Technology 144 (2022). https://doi.org/10.1115/1.4054366

[14] F.R. Cao, H. Ding, Y. Li, G. Zhou, I.Z. Cui, Superplasticity, dynamic grain growth and deformation mechanism in ultra-light two-phase magnesium-lithium alloys, Mater. Sci. Eng. A 527 (2010) 2335-2341. https://doi.org/10.1016/j.msea.2009.12.029

[15] S.-J. Kim, C. Lee, J. Koo, J. Lee, Y. Lee, D. Kim, Improving the room-temperature formability of a magnesium alloy sheet by texture control, Mater. Sci. Eng. A 724 (2018) 156-163. http://dx.doi.org/10.1016/j.msea.2018.03.084

[16] K. Suzuki, Y. Chino, X. Huanng, M. Yuasa, M. Mabuchi, Enhancement of Room Temperature Stretch Formability of Mg-1.5 mass%Mn Alloy by Texture Control, Mater. Trans. 54 (2013) 392-398. https://doi.org/10.2320/matertrans.M2012312

[17] Y. Nakayama, T. Naka, T. Uemori, I. Shimizu, Temperature and Processability of Magnesium Alloy AZ31 on Rectangular Cup Deep Drawing, Key Eng. Mater. 535/536 (2013) 326-32. https://doi.org/10.4028/www.scientific.net/KEM.535-536.326

[18] K. Bhardwaj, P. Sandeep, T. Saurabh, B. Santosh, Corrosion and Mechanical Aspects of Friction Stir Welded AA6061 Joints: Effects of Different Backing Plates, J. Mater. Eng. Perform. 32 (2023) 10817-10833. https://ui.adsabs.harvard.edu/link_gateway/2023JMEP...3210817K/doi:10.1007/s11665-023-07900-x

[19] B. Wang, P. Zhu, Y. Cao, L. Zhou, P. Xue, L. Wu, Effects of different friction stir welding processes on residual stress and deformation of Ti62A alloy joints, J. Mater. Res. Tech. 26 (2023) 6096-6107. https://doi.org/10.1016/j.jmrt.2023.08.308

[20] T. Li, X. Xie, J. Xu, R. Li, K. Qi, X. Zhang, H. Yue, Y. Zhao, L. Lei, Research on AZ31 Mg alloy/22MnB5 steel pinless friction stir spot welding process and interfacial temperature field simulation, J. Mater. Res. Tech. 26 (2023) 3710-3725. https://doi.org/10.1016/j.jmrt.2023.08.169

[21] Y. Lee, S. Kim, S.-Y. Park, J. Yoo, Y. Moon, Friction effect of surface treated tools used for warm forming of Mg alloy sheets, Int. J. Precision Eng. Manuf. 15 (2014) 2631-2637. https://doi.org/10.1007/s12541-014-0637-x

[22] F. Tamashiro, H. Hamasaki, F. Yoshida, Equi-Plastic Work Locus of 5000 Series Aluminum Alloy Sheet at Warm Temperature, Key Eng. Mater. 725 (2017) 695-699. http://dx.doi.org/10.4028/www.scientific.net/KEM.725.695

[23] P. Muthuswamy, Investigation on sustainable machining characteristics of tools with serrated cutting edges in face milling of AISI 304 Stainless Steel, Procedia CIRP 105 (2022) 865-871. https://doi.org/10.1016/j.procir.2022.02.143

[24] Information on https://www.jssa.gr.jp/english/

[25] M. Toit, H. G. Steyn, Comparing the Formability of AISI 304 and AISI 202 Stainless Steels, J. Mater. Eng. Perform. 21 (2012) 1491-1495. http://dx.doi.org/10.1007/s11665-011-0044-8